Sub-daily rainfall extremes in the Nordic–Baltic region

Jonas Olsson [ID][a,*], Anita Verpe Dyrrdal[b], Erika Médus[c], Johan Södling[d], Svetlana Aņiskeviča[e], Karsten Arnbjerg-Nielsen [IWA][f], Eirik Førland[b], Viktorija Mačiulytė[g], Antti Mäkelä[h], Piia Post[i], Søren Liedke Thorndahl [IWA][j] and Lennart Wern[k]

[a] Research & Development, Swedish Meteorological and Hydrological Institute, Norrköping, Sweden
[b] Research & Development, Norwegian Meteorological Institute, Oslo, Norway
[c] Climate System Research, Finnish Meteorological Institute, Helsinki, Finland
[d] Professional Services, Swedish Meteorological and Hydrological Institute, Norrköping, Sweden
[e] Forecasting and Climate Department, Latvian Environment, Geology and Meteorology Centre, Riga, Latvia
[f] Department of Environmental Engineering, Technical University of Denmark, Lyngby, Denmark
[g] Institute of Geosciences, Vilnius University, Vilnius, Lithuania
[h] Weather and Climate Change Impact Research, Finnish Meteorological Institute, Helsinki, Finland
[i] Institute of Physics, University of Tartu, Tartu, Estonia
[j] Department of the Built Environment, Aalborg University, Aalborg, Denmark
[k] Core Services, Swedish Meteorological and Hydrological Institute, Norrköping, Sweden
*Corresponding author. E-mail: jonas.olsson@smhi.se

[ID] JO, 0000-0001-5907-4061

ABSTRACT

Short-duration rainfall extremes are associated with a range of societal hazards, notably pluvial flooding but in addition, e.g., erosion-driven nutrient transport and point-source contamination. Fundamental for all analysis, modelling and risk assessment related to short-duration rainfall extremes is the access to and analysis of high-resolution observations. In this study, sub-daily rainfall observations from 543 meteorological stations in the Nordic–Baltic region were collected, quality-controlled and consistently analyzed in terms of records, return levels, geographical and climatic dependencies, time of occurrence of maxima and trends. The results reflect the highly heterogeneous rainfall climate in the region, with longitudinal and latitudinal gradients as well as local variability, and overall agree with previous national investigations. Trend analyses in Norway and Denmark indicated predominantly positive trends in the period 1980–2018, in line with previous investigations. Gridded data sets with estimated return levels and dates of occurrence (of annual maxima) are provided open access. We encourage further efforts towards international exchange of sub-daily rainfall observations as well as consistent regional analyses in order to attain the best possible knowledge on which rainfall extremes are to be expected in present as well as future climates.

Key words: climate, precipitation, short-duration

HIGHLIGHTS

- Sub-daily annual rainfall maxima have been collected from national observation networks in the Nordic–Baltic region, including a total of 543 stations.
- A consistent regional analysis of records, return levels, geographical and climatic dependencies, time of occurrence of maxima and trends is performed.
- Gridded data sets with return levels and time of occurrence are provided open access.

GRAPHICAL ABSTRACT
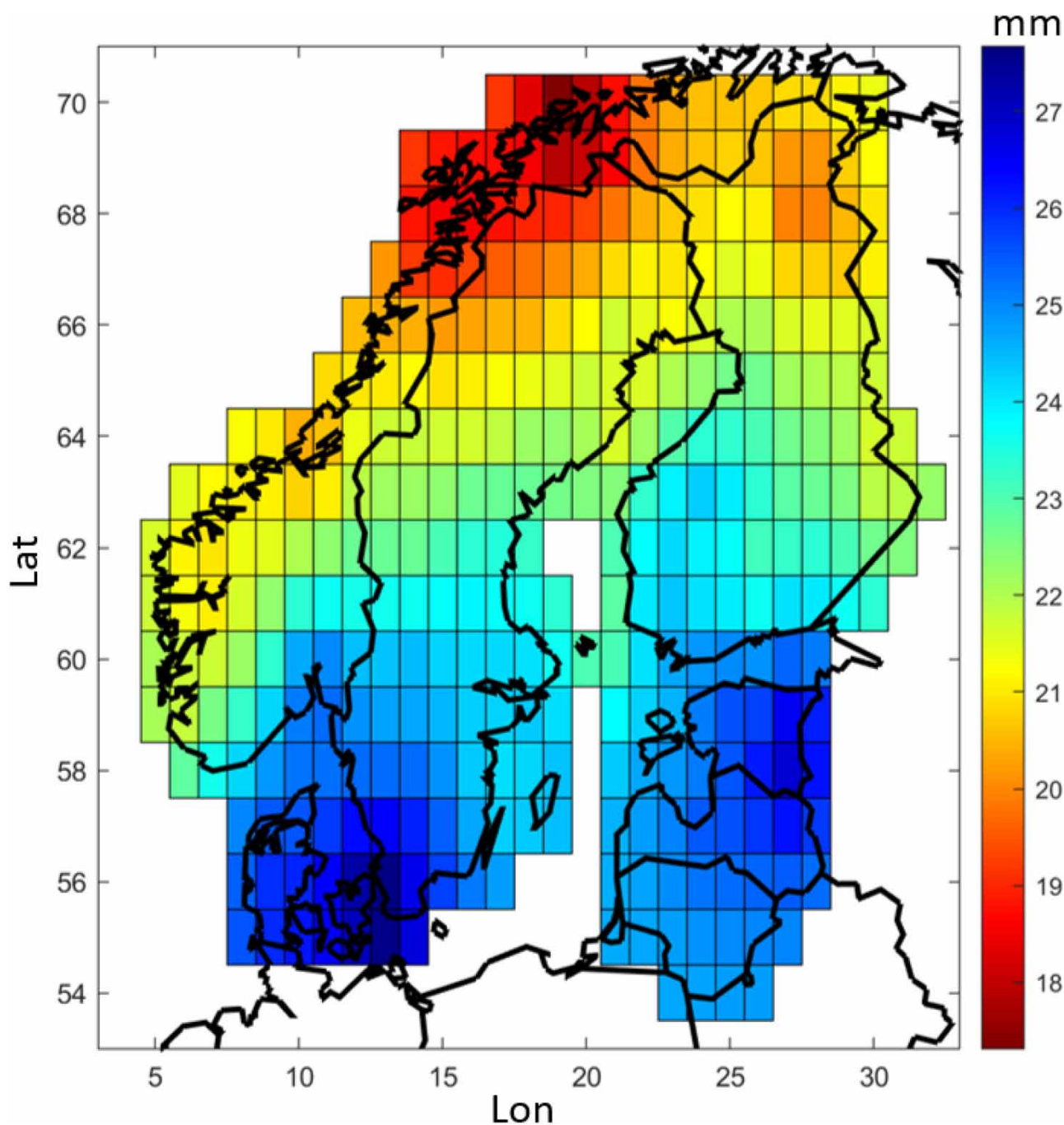
INTRODUCTION

Rainfall extremes at sub-daily, or even sub-hourly, time scales are associated with a range of societal hazards. A main hazard is pluvial flooding, when high or extreme rainfall intensities exceed the drainage capacity and water is rapidly being conveyed and concentrated into low-lying areas. Urban environments with a large fraction of impervious surface are particularly prone to pluvial flooding, and also particularly vulnerable to damage considering the high density of people, buildings and activities (e.g. Willems *et al.* 2012). However, pluvial flooding may also happen in natural environments, e.g., when slopes are steep and soils are thin. Besides pluvial flooding, short-duration rainfall extremes are associated with landslides and debris flow as well as risks associated with water quality. The latter include, e.g., erosion-driven nutrient transport and point-source contamination.

Concerning the Nordic–Baltic region, there are several historical examples of severe flooding as a result of short-duration rainfall extremes. The most well-known case is that in Copenhagen 2 July 2011 when a cloudburst generating >125 mm of rainfall in a few hours, peaking at >30 mm during 10 min, caused damages (insurance claims) exceeding 800 MEUR (Arnbjerg-Nielsen *et al.* 2015). A list of recent high-damage pluvial events in the region is provided by Dyrrdal *et al.* (2021). A main cause of concern is that short-duration rainfall extremes are intensifying as a function of global warming (IPCC 2021). Empirical evidence in the region is still limited, partly related to a lack of long enough time series, but positive trends have been found (e.g. Arnbjerg-Nielsen 2006; Sorteberg *et al.* 2018). This evolution implies a need for better support for society with respect to cloudbursts and pluvial floods, both in terms of short-term forecasts (for early warning and situation awareness) and long-term projections (for planning and adaptation). A key to attaining this support is the rather recent development of high-resolution convection-permitting atmospheric models, that have proved to greatly improve the simulation of local high-intensity rainfall. This type of model has been used for operational forecasting in the region for a few years (Müller *et al.* 2017) and very recently for climate projections (Lind *et al.* 2020).

Fundamental for all analysis, modelling and risk assessment related to short-duration rainfall extremes is the access to high-resolution observations. Historical quality-controlled observations are needed, e.g., for development of statistics for design (e.g. intensity–duration–frequency (IDF) curves), for post-event analyses following pluvial floods and for development and evaluation of atmospheric models. Real-time observations are needed, e.g., for situation awareness during flood events and for initialization of hydrological or hydraulic flood models. The most reliable observation source is the rainfall gauge, which is generally of weighing or tipping-bucket type. Different gauge networks exist, e.g., national networks operated by weather services, regional or local networks operated by cities or municipalities and commercial networks collecting citizen observations. Weather radar has the advantage of providing a high spatial and temporal resolution over a large area, but requires a dense rain gauge network for calibration in order to attain accurate estimation of rainfall intensity. Several types of radar exist including C-band, X-band and Micro Rain Radar (e.g. Thorndahl *et al.* 2017; Sokol *et al.* 2021). Another technique being explored is to measure rainfall intensity as a function of signal attenuation in commercial microwave link networks (e.g. von Scherling *et al.* 2021).

Despite the evident importance of high-resolution sub-daily rainfall observations, only a few attempts have been made to collect and analyze this type of observation across national borders. This lack of multi-national data complicates, e.g., climate model evaluation, as different national observational data bases (or statistics) have to be retrieved, processed and combined (e.g. Berg *et al.* 2019). Besides being time consuming, it becomes challenging and uncertain because of differences in, e.g., the sensors, resolutions and processing methods used in different countries. On the global scale, sub-daily observations are available through the ISD (Integrated Surface Database; Smith *et al.* 2011), with ~8,000 stations but many with only short records (Lewis *et al.* 2019). A major collection effort was made by Lewis *et al.* (2019), who compiled the GSDR (Global Sub-Daily Rainfall) data set containing observations from almost 24,000 stations worldwide with an average record length of 13 years. A subset of GSDR is open access. On the European scale, Poschlod *et al.* (2021) very recently compiled observation-based estimates of the local 10-year rainfall in 16 countries, including the Nordic countries (except Iceland). The methods and procedures used to estimate the 10-year rainfall from observations differ between the different countries.

The objectives of this study are to collect sub-daily (hourly) rainfall observations in the Nordic–Baltic region, turn them into a quality-controlled data base, perform a consistent statistical analysis, present and interpret the results, and finally provide open access to key output. The finally analyzed data base comprises 370 stations with record lengths between 6 and 38 years. The results highlight geographical variations over the region in terms of both (*i*) extreme rainfall accumulations for different (sub-daily) durations and (*ii*) their time of occurrence (i.e. day of year (doy)). The latter aspect is seldom considered in analyses of short-duration rainfall extremes, although it is a fundamental characteristic closely related to the physical processes involved. Gridded data representing both these aspects are provided with open access as a source for, e.g., climate model evaluation and potential regional harmonization of rainfall statistics and analysis methods.

STUDY AREA AND DATA

Climate

The Nordic–Baltic domain under study (Figure 1) exhibits pronounced climatic gradients, in terms of both temperature and precipitation and in both longitudinal and latitudinal directions. This heterogeneity is reflected in the Köppen-Geiger climate classification. In the recent update performed by Beck *et al.* (2018), the domain includes no less than three out of the five
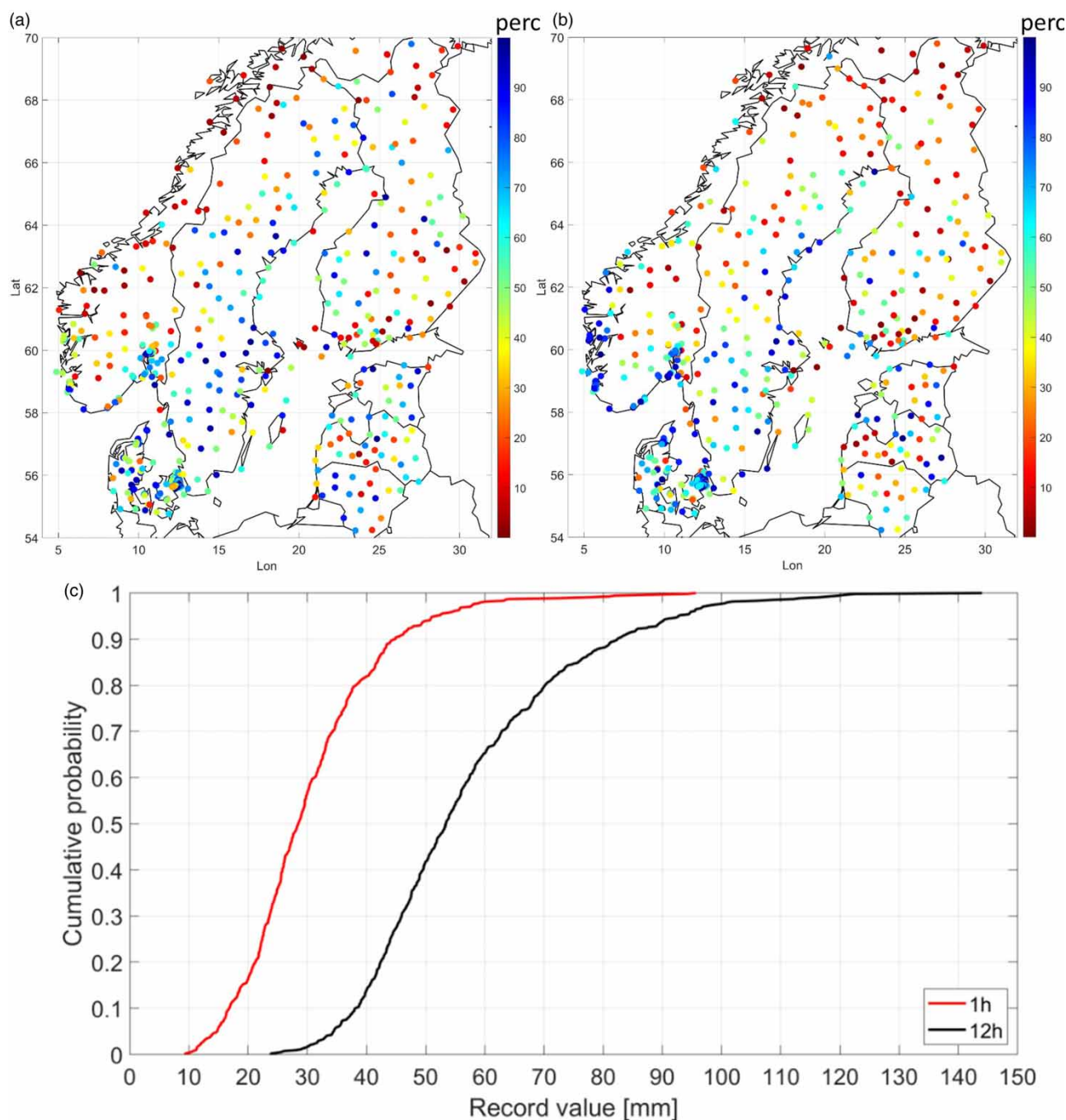
Figure 1 | Record values, i.e., the highest observed values, of the following durations: (a) 1 h and (b) 12 h (zoom-ins on DK are available in Supplement, Figure S1). (c) The colours represent the percentile (perc) of the entire frequency distributions. Please refer to the online version of this paper to see this figure in colour: http://dx.doi.org/10.2166/nh.2022.119.

main Köppen-Geiger classes: cold, polar and temperate. Most of the domain – including most of Norway, Sweden north of ∼60 °N and virtually all of Finland – belongs to class Dfc, cold climate without dry season and with cold summers. Central Norway as well as the northernmost part of the Scandinavian mountains are classified as polar tundra climate (ET). The Baltic states, Sweden south of ∼60 °N, north-eastern Denmark as well as southernmost Norway and Finland belong to class Dfb, cold climate without dry season and with warm summers. Finally, south-western Denmark is classified as having a temperate climate without dry season and with warm summer (Cfb).

In terms of precipitation, solid precipitation is frequent during the winter half-year in the northern part of the domain, especially in mountainous regions and in the northern continental parts. Most of the annual rainfall generally occurs during summer and autumn, with spring being drier. Annual precipitation totals vary widely within the domain, by a factor of 10 from ~400 mm in northern Finland up to 4,000 mm (or even more) in western Norway, an area frequently exposed to storms travelling with westerly winds along the North Atlantic jet stream (see further Dyrrdal *et al.* 2021). Throughout the year precipitation is generated in connection with the passage of cyclonic fronts, which are formed along the polar front at the interface between cold and warm air masses. Short-duration rainfall extremes occur primarily in the warm season, especially July and August. These extremes are generally associated with convection, either in the form of single thunderstorms or embedded in mesoscale convective systems.

Observations

Sub-daily observations from a total of 543 stations in the Nordic–Baltic domain were collected and used in the study; their locations are shown in Figure 1 and an overview is presented in Table 1. Most of the observations are openly available and they have been collected as a joint effort within the Nordic Framework for Climate Services (NFCS). Other sub-daily observations are available in several countries, but not included here because of, e.g., limited quality control or insufficient temporal resolution.

In the following, some details of the observations and devices are given, with references to more information (when available).

- Denmark (DK): Tipping-bucket gauges of type RIMCO that register the number of tips every minute, each tip representing 0.2 mm of rainfall, are used. A thermo-controlled heating system has been used since the mid-1990s. Quality control is performed both automatically and manually (see further Jørgensen *et al.* 1998).
- Estonia (EE): Since 2003, tipping-bucket gauges of type Vaisala RG13H have been recording precipitation, with 0.2 mm volume resolution and time-of-tip recording. In 2010 (2006 in Tallinn), these gauges were replaced by type Vaisala VRG101 weighing gauges (0.1 mm resolution) with heating and wind shield in order to accurately measure solid precipitation as well. Until the end of 2010, the temporal resolution was 1 h, and since then the data were recorded with a 10-min interval. In this study, 1-h gauge data were used to obtain a longer time series (see further Alber *et al.* 2015).
- Finland (FI): Between 2001 and 2013, weighing gauges of type OTT Pluvio1 were used to observe precipitation with a 1-h time step and a volume resolution of 0.01 mm. The gauges were heated and equipped with a wind shield. Shielded Vaisala

Table 1 | Overview of gauges and observations used in the study

	Gauge model and type[a]	Time step(s)	Start	N_{tot}	Open	1981–1999 N>10 years	2000–2018 N>10 years
DK	RIMCO (TB)	1 min	1979	109	No	34	102
EE	Vaisala RG13H (TB), Vaisala VRG101 (W)	1 h	2004	18	Yes[b]	–	16
FI	OTT Pluvio1 and 2 (W), Vaisala VRG101 (W)	10 min, 1 h	2001	108	Yes[c]	–	51
LV	OTT Pluvio2 (W)	1 h	2005	28	Yes[d]	–	2
LT	Vaisala VRG101 (W)	1 h	2013	18	No	–	–
NO	Plumatic (TB), Lambrecht 1518 H3 (TB) Geonor T-200B (W)	1 min 10 min, 1 h	1967 1994	74 60	Yes[e]	13	92
SE	Geonor T-200B (W)	15 min	1996	128	Yes[f]	–	107
TOT				543		47	370

N_{tot} refers to the total number of stations in the data set. N>10 years refers to the number of stations with more than 10 years of data used in the GEV analysis.
[a]TB=tipping-bucket gauge, W=weighing gauge.
[b]http://www.ilmateenistus.ee/kliima/ajaloolised-ilmaandmed/.
[c]https://en.ilmatieteenlaitos.fi/download-observations (from 2010).
[d]https://www.meteo.lv/meteorologija-datu-meklesana/?nid=461.
[e]https://seklima.met.no/.
[f]https://www.smhi.se/data/.

VRG101 gauges were also used in this period. Between 2012 and 2015, the gauges were replaced by type OTT Pluvio2 with a modified wind shield, and the time step was shortened to 10 min.

- Latvia (LV): During the period of study, gauges of type OTT Pluvio2 were used. All gauges have a wind shield. Measurements are made with a 1-min time step but only 1-h accumulations are stored.
- Lithuania (LT): Since 2013, precipitation has been measured by Vaisala VRG101 weighing gauges providing 1-h accumulations (also 10-min intensity). Hourly data quality control is performed automatically and manually. Daily and monthly precipitation data must be complete sequences, otherwise amounts are not calculated.
- Norway (NO): Until the late 1990s, observations were made by tipping-bucket gauges of type Plumatic, with a 0.2 mm volume resolution and a 1-min time step. From that time, these gauges were all successively replaced by the Lambrecht 1518 H3 tipping-bucket pluviometer with 0.1 mm and 1-min resolutions (Lutz *et al.* 2020). Unheated tipping-bucket gauges are not operative in the winter season. Since the mid-1980s, all-year operating Geonor T-2008 weighing gauges (Bakkehøi *et al.* 1985) with windshield were included in the sub-daily network. The temporal resolution is presently 10 min.
- Sweden (SE): Observations are made by weighing type gauges Geonor T-200B, with heating and wind shield. Additionally, a thin layer of oil is added to impede any evaporation. The data are stored as 15-min accumulations with a 0.1 mm volume resolution (see further Olsson *et al.* 2019).

Besides the gauge observations, estimates of average temperature and total precipitation during summer were used to investigate links between these climate features and sub-daily rainfall extremes (see Methods). These temperature and precipitation data were retrieved from the ERA5 meteorological reanalysis (Hersbach *et al.* 2020). For the analyses, ERA5 data from the grid cell (resolution 31 km × 31 km) covering each gauge were averaged or accumulated over the summer season, June–August (JJA).

Quality control, retrieval and correction of annual maxima

Each institute was responsible for calculating annual maxima (AM) from the continuous time series. As the institutes use different methods and practices for quality control, no common quality control was applied but we assume that the internal control is accurate. Some institutes have automatic quality control, in some it is a manual procedure and in some both automatic and manual procedures are used. In the extraction of AM, different requirements have been applied concerning the maximum number of missing time steps allowed in a certain year, season or month. In some cases, subjective judgement was used to remove suspicious AM. In total, we have performed as much quality assurance as was possible within the resources for the study and we assume that the final data are sufficiently accurate for the analyses performed.

Retrieval of AM for durations 1, 3, 6 and 12 h from the original time series was performed in the conventional way. Generally, a moving time window of length D was moved forward one time step at a time, where the time step ranges between 1 min and 1 h in the observations (Table 1). Each time the rainfall depth in the time steps within the window was accumulated, and finally the highest accumulation in each year was kept.

Finally, a correction was applied to account for the time step in the original time series. Observations collected at fixed time intervals will most likely miss true maximum accumulations (e.g. Young & McEnroe 2003). As an example, it is very unlikely that fixed 1-h accumulations (e.g. between every whole hour) from a certain rainfall event will capture the actual 1-h maximum during the event, that would have been found by, e.g., moving window analysis of 1-min observations during the event (see Olsson *et al.* 2019).

To correct for this effect, multiplicative factors were applied to some of the AM. Most of the correction was applied to the 1-h maxima from time series with a time step >1 min (observations with a 1-min time step, only available from DK, are assumed not to require any correction). Annual 1-h maxima from observations with a fixed 1-h time step (Estonia, Finland, Latvia and Norway) were multiplied by 1.14, observations with 15-min time step by 1.04 (Sweden) and observations with 10-min time step by 1.02 (Finland). Furthermore, 3-h maxima were generally (except in Denmark and Sweden) corrected using a factor 1.03. The values of the correction factors were determined based on both published values (e.g. Young & McEnroe 2003; WMO 2009) and analyses of 1-min observations performed within this study.

Whereas it is well-known that short-duration rainfall extremes in the domain generally occur in summer, we are not aware of any investigation of regional patterns in their time of occurrence. Therefore, besides the value of the AM, their dates of occurrence were registered and collected.

METHODS

We primarily used Generalized Extreme Value (GEV) analysis (Coles 2001) to estimate the return levels at sub-daily time-scales. As the analyzed time periods were rather short, 11–19 years, we assumed that the distribution of AM is stationary in time. This assumption was tested using the Kwiatkowski–Phillips–Schmidt–Shin (KPSS) test.

Return levels of rainfall extremes were estimated by fitting the GEV distribution to annual precipitation maxima. The cumulative distribution function of the GEV:

$$F(x) = \exp\left(-\left(1 + \xi\left(\frac{x - \mu}{\sigma}\right)^{-1/\xi}\right)\right), \xi = 0 \tag{1}$$

$$= \exp\left\{-\exp\left[-\left(\frac{x - \mu}{\sigma}\right)\right]\right\}, \xi = 0$$

where in our case x is the accumulated rainfall over a certain duration, and is defined by three parameters (location μ, scale σ and shape ξ). The parameters were estimated with L-moments (Hosking 1990) which is a preferred method over maximum likelihood when the sample size is small (Hosking & Wallis 1987). The return levels for different return periods can be estimated from the quantile function:

$$F^{-1}(p) = \mu + \frac{\sigma}{\xi}\{[-\ln(p)]^{-\xi} - 1\}, \ \xi \neq 0 \tag{2}$$

$$= \mu - \sigma \times \ln(-\ln(p)), \ \xi = 0$$

where $p = F(x)$. We computed return levels for durations (i.e. accumulation periods) 1, 3, 6 and 12 h and for return periods 5, 10 and 20 years. The goodness-of-fit was checked by the Kolmogorov–Smirnov test that compares the empirical distribution function with a specified distribution function. In addition to the GEV, the Gumbel distribution was tested.

From the estimated return levels in the gauge locations, grids were constructed by inverse distance weighting with the power parameter optimized to a value of 2 by visual judgement. A grid resolution of 1° × 1° was selected as this generates ~330 grid cells in the domain (excluding the sea and neighbouring countries), a number that well matches the number of gauges used in the 2000–2018 analysis (370; Table 1).

In the domain, several attempts have been made to relate return levels of sub-daily rainfall to geographical and hydro-meteorological predictors. In Sweden, an approach relating IDF statistics to average summer temperature and total summer precipitation has been developed and refined (Dahlström 1979, 2021). In Denmark, several predictors have been used since the first regional model was established in 1999. The mean annual precipitation has always been used to predict the rate of extreme events, but with different predictors of the size of the events. Currently, the mean extreme daily precipitation derived from an independent data set is used to supplement the mean annual precipitation as covariate (Madsen et al. 2017). In Dyrrdal et al. (2015), return levels for hourly rainfall in Norway are computed using different predictors on a high-resolution national grid in a spatial model. They found average summer temperature to be amongst the best predictors of heavy sub-daily rainfall.

Here, we present only a limited assessment of the relationship between return levels and four potential predictors: latitude, longitude, average summer (JJA) temperature and total summer precipitation. We expect latitude to reflect primarily temperature dependence, whereas longitude generally reflects more complex combinations of meteorological and geographical characteristics. The assessment is made only in terms of scatter plots and visual inspection without any further mathematical or statistical analysis.

Concerning the dates of occurrence of the AM, the median date in each gauge was calculated, plotted and analyzed. Furthermore, 1° × 1° grids were made in the same way as for the return levels.

As seen in Table 1, in Denmark and Norway, we have observations since 1981 from a number of stations, which allows for a limited trend analysis. In this analysis, we compare estimated return levels from period 1981–1999 with estimates from our main period 2000–2018.

RESULTS

In Figure 1, the record values in each station are shown, i.e., the highest observed value in the time series. In this analysis all collected data are used which means that the available time period differs between stations. Note that (*i*) as a time step correction was applied (see Methods) the values may differ from established national (un-corrected) record values and (*ii*) new records in some cases have occurred after the period analyzed here. For improved clarity, the colour legend in the maps (Figure 1(a) and 1(b)) represents the percentile in the cumulative distribution of all record values (Figure 1(c)). For example, green represents the median and at duration 1 h (Figure 1(a)) this corresponds to a rainfall depth of 28 mm (Figure 1(c)).

At duration 1 h, the values range from 9.4 to 95.6 mm with ~90% between 15 and 50 mm. The highest value was observed in Latvia 29 July 2014, during a cloudburst that caused considerable damage to the local municipality. It may be mentioned that a manual analysis of the event suggests that the correction applied (see Methods) in this case led to some overestimation, and that the actual value was ~8 mm lower. The second highest value, 94.2 mm, was observed in Denmark during the devastating cloudburst over Copenhagen 2 July 2011. There are in total 11 observations exceeding 60 mm in 1 h; seven in Denmark, two in Sweden and one each in Latvia and Estonia. The highest 1-h value observed in Finland is 59.2 mm, in Norway 54.9 mm and in Lithuania 46.7 mm. On the lower end, two stations have a record below 10 mm in 6 h and both are located in Sweden. The map (Figure 1(a)) shows that the highest records are generally found in Denmark, southern Sweden and the Baltic states, but that very high values have occurred also in the very north of the domain.

At duration 12 h, the values range from 23.8 to 144.0 mm with ~90% between 35 and 95 mm. The highest value was observed in south-western Norway on 5 October 1983, in connection with a deep low pressure, and the huge rainfall amounts caused severe flooding and damage in the Odda valley. Several stations have records around 120 mm in 12 h, including observations from the large 1-h events in Latvia and Denmark described above. Two stations have 12-h records below 25 mm in 12 h, one located in Finland and one in Sweden. The highest values are generally found along the western and southern coast of Norway, Denmark, along the Swedish coast and in the Baltic states (Figure 1(b)). Only very few high 12-h records have been observed in the northern half of the domain.

Based on the KPSS test, most of the time series were found to be stationary during 1980–1998 (>95% of the stations) and 2000–2018 (>97%). Concerning the GEV fitting, no station was rejected by the Kolmogorov–Smirnov test but all can be assumed to follow a GEV distribution. As described in Methods, the Gumbel distribution was also tested, but as the GEV distribution exhibited a distinctly better goodness-of-fit to the empirical values, we focus on GEV estimates in the following. The GEV shape parameter ξ is with a few exceptions in the range $-0.5 < \xi < 0.5$. In the Supplement, histograms of ξ are provided (Figure S2) as are maps showing the spatial distribution (Figure S3).

The estimated 10-year return levels for durations 1, 3, 6 and 12 h are shown in Figure 2. We here present results for return period 10 years, but the spatial patterns and geographical dependencies are overall similar for return periods 5 and 20 years.

At duration 1 h (Figure 2(a)), the highest values, up to >40 mm in 1 h, are located in eastern Denmark, but in the map these dots are largely masked by other dots in the very densely gauged Denmark. High values are also found in southern Norway, southern Sweden and the Baltic states, in line with the pattern of the 1-h records (Figure 1(a)), and in southern Finland with values up to ~35 mm in 1 h. Low values generally appear in north-western Norway, northern Sweden and northern Finland.

For longer durations, there is a gradual transition through 3 and 6 h to the pattern seen at duration 12 h (Figure 2(d)). Here, the highest values are concentrated mainly to the western and southern coast of Norway. High values appear also in eastern Denmark, although less visible in the map. In contrast to the pattern at 1 h (Figure 2(a)), at 12 h the 10-year values in southern Finland and in the Baltic states are relatively low.

In Figure 3, interpolated 1° × 1° grids representing the 10-year values at durations 1 and 12 h are shown. We emphasize that a grid cell value does not represent a spatial average value but a point value in an arbitrary location inside the grid cell. Note that the colour legend in Figure 3 differs from the legend used in Figure 2. These data are provided as open access with this paper, see further Data availability statement.

The grid at 1 h (Figure 3(a)), interpolated from the point values in Figure 2(a), clearly shows the 'hot spot' in Denmark and south-western Sweden as well as the distinct latitudinal dependence. The maximum value in the south-west, 27 mm, is 50% larger than the minimum value in the north (18 mm). At longer durations, the latitudinal dependency is gradually replaced by a gradient from south-west to north-east, still manifested in a 50% difference between the maximum and minimum values.

As evident from Figures 2(a) and 3(a), the estimated 1-h 10-year values have a dependence on latitude (Figure 4(a)). Although the scatter is pronounced, with values of 20 mm occurring both at the lowest and at the highest latitudes, the highest
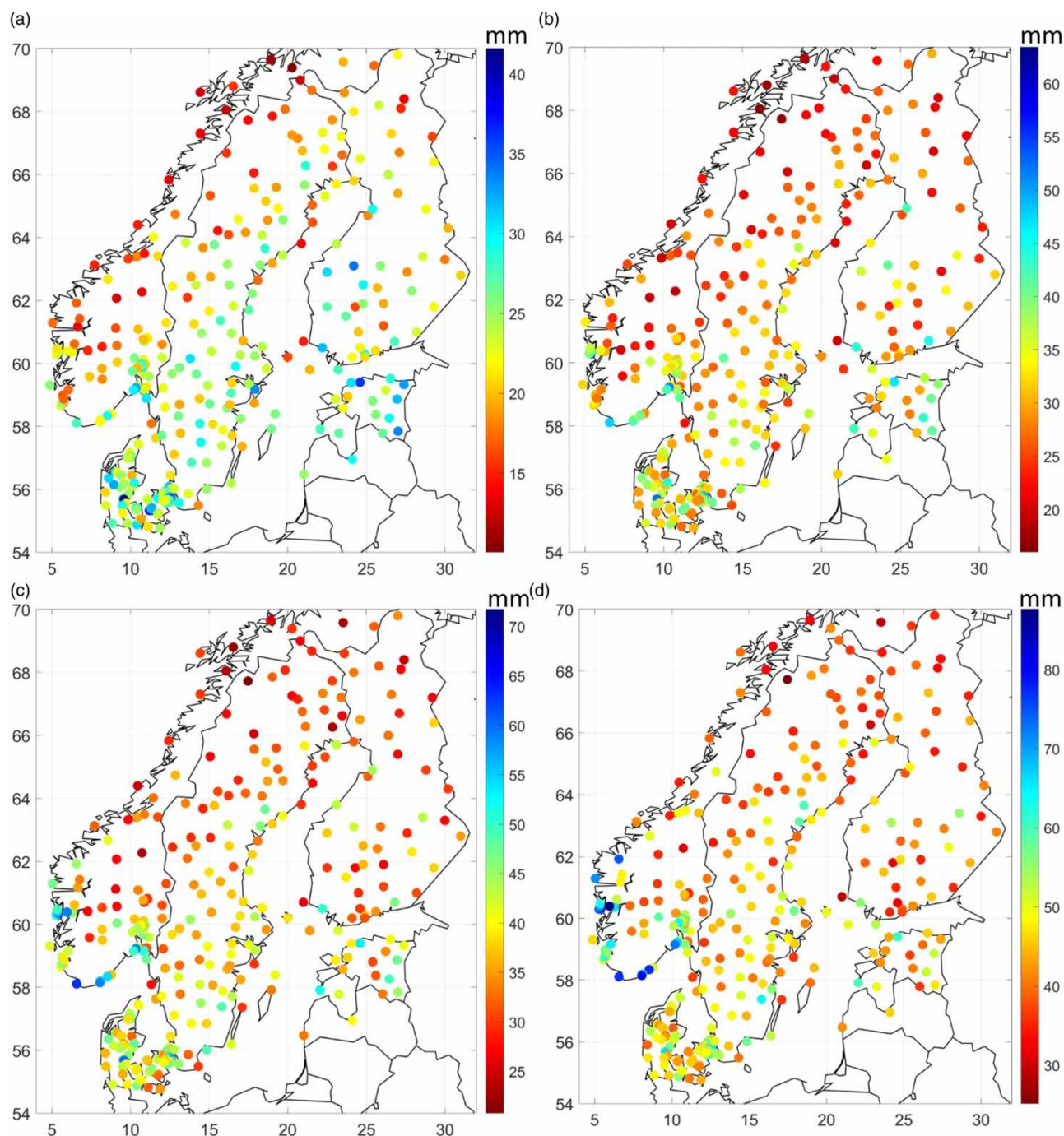
Figure 2 | Estimated 10-year rainfall (mm) for the following durations: (a) 1 h, (b) 3 h, (c) 6 h and (d) 12 h (zoom-ins on DK are available in Supplement, Figure S4).

10-year values occur at the lowest latitude and vice versa. Note that the many stations in Denmark are reflected in a vertical line between latitudes 55 °N and 56 °N. At duration 12 h (Figure 4(b)), a clear dependence still exists although the highest values now occur close to latitude 60 °N, which reflects the 'maximum area' in western Norway (Figure 3(d)). No dependence of the 1-h 10-year value on longitude was found (Figure 4(c)), in line with the pattern in Figure 3(a). At duration 12 h, however, a longitude dependence is clear in line with Figure 3(d).

As expected from the latitude dependence, both the 1-h (Figure 5(a)) and the 12-h (Figure 5(b)) 10-year rainfall has a corresponding dependence on mean summer temperature, with a similar scatter. Figure 5(a) and 5(b) are very close to inverted
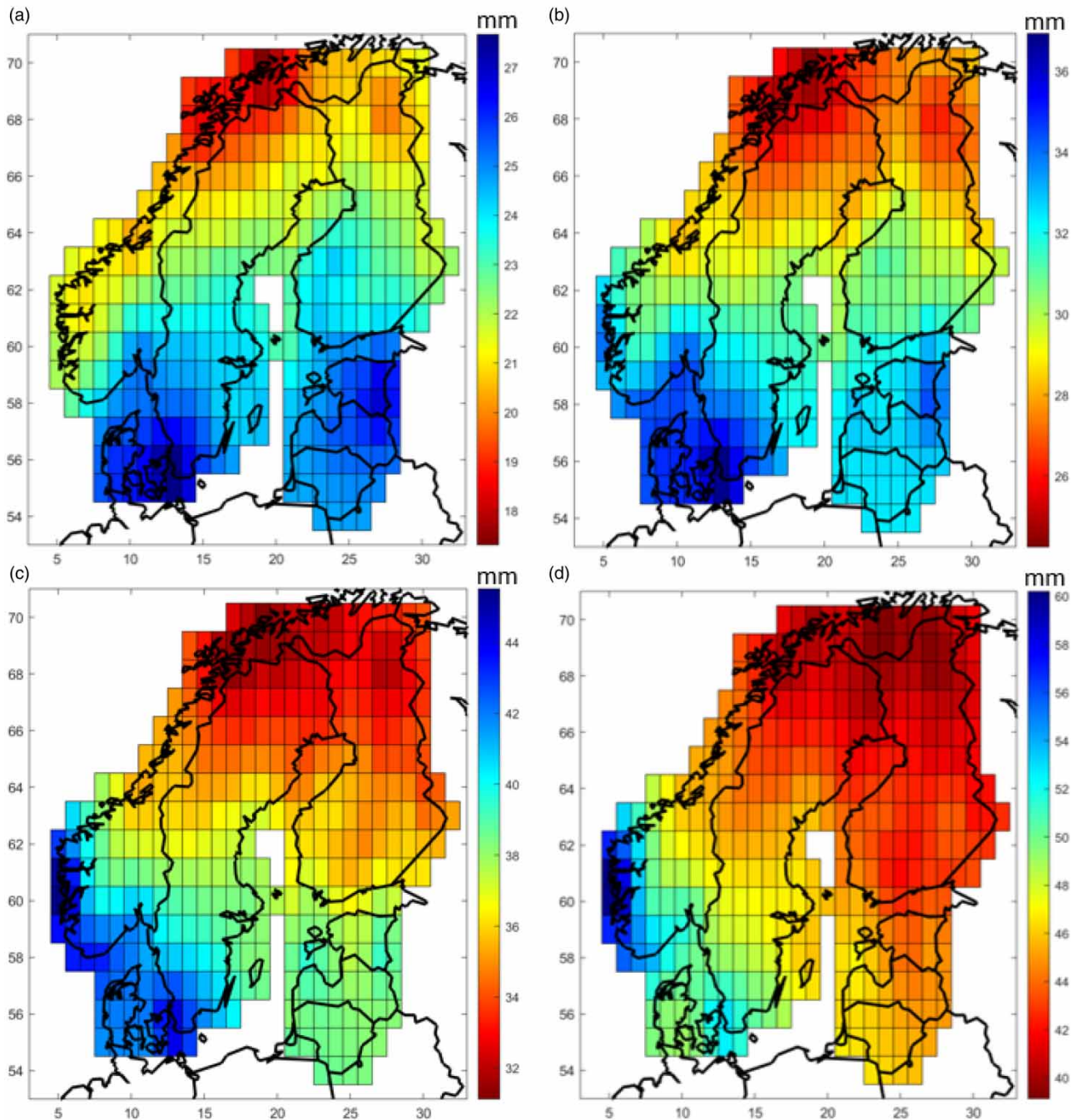
Figure 3 | Gridded (interpolated) 10-year rainfall (mm) for the following durations: (a) 1 h, (b) 3 h, (c) 6 h and (d) 12 h.

versions of Figure 4(a) and 4(b). Any dependence on mean summer precipitation can, however, not be found (Figure 5(c) and 5(d)). We only note that the lowest 1-h values occur for stations with very low summer precipitation (Figure 5(c)) and highest 12-h values occur for stations with very high summer precipitation.

In Figure 6, the maximum dates of each station are shown, i.e., the median date of the dates corresponding to the extracted AM. Similar to Figure 1, the colour legend in the maps (Figure 6(a) and 6(b)) represents the percentile in the cumulative distribution of all maximum dates (Figure 1(c)).

At duration 1 h, the median dates range between 180 (late June) and 270 (late September). The central 90% of the dates occur approximately from mid-July to mid-August (Figure 6(c)). Stations with very early dates (≤0.05) are spread more or
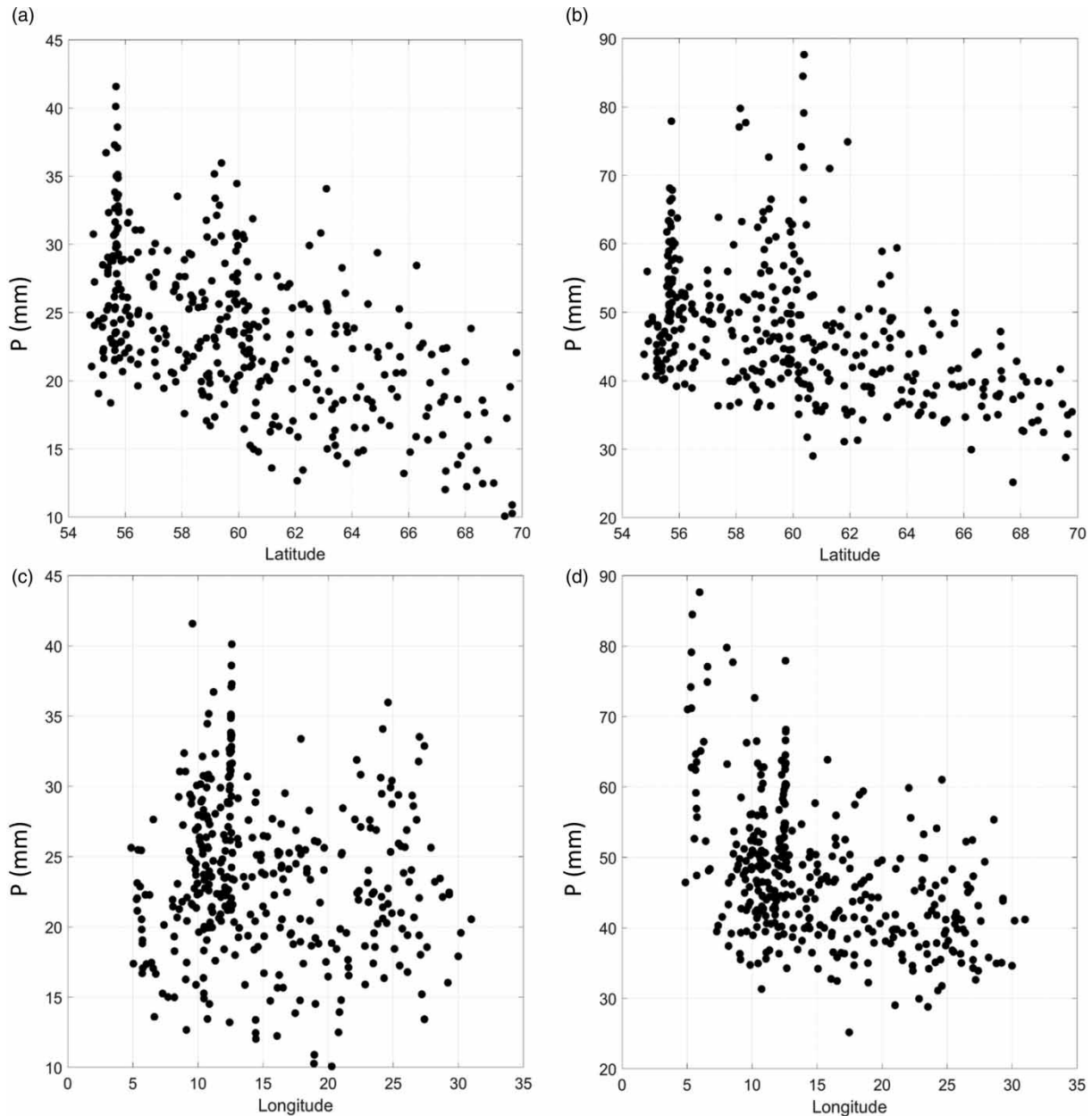
Figure 4 | Estimated 10-year rainfall P as a function of latitude (°N) for the following durations: (a) 1 h and (b) 12 h and as a function of longitude (°E) for the following durations: (c) 1 h and (d) 12 h.

less all over the domain, except western Norway. Stations with very late dates ($\geqslant$0.95) are mainly located in western Norway, Denmark, southern Finland and the Baltic states (Figure 6(a)). At duration 12 h, the distribution of dates has a wider spread, from mid-June to late October, with the majority between early July and early September. In particular, there is a shift towards later dates (Figure 6(c)). The spatial pattern (Figure 6(b)) has many similarities with the pattern found at 1 h (Figure 6(a)) but there are fewer very late dates in the eastern part of the domain and more in the western part. A longitudinal dependence is suggested, with early dates in the east and late dates in the west.

In Figure 7, interpolated 1° × 1° grids representing the maximum dates at durations 1 and 12 h are shown. These data are provided as open access with this paper, see further Data availability statement.
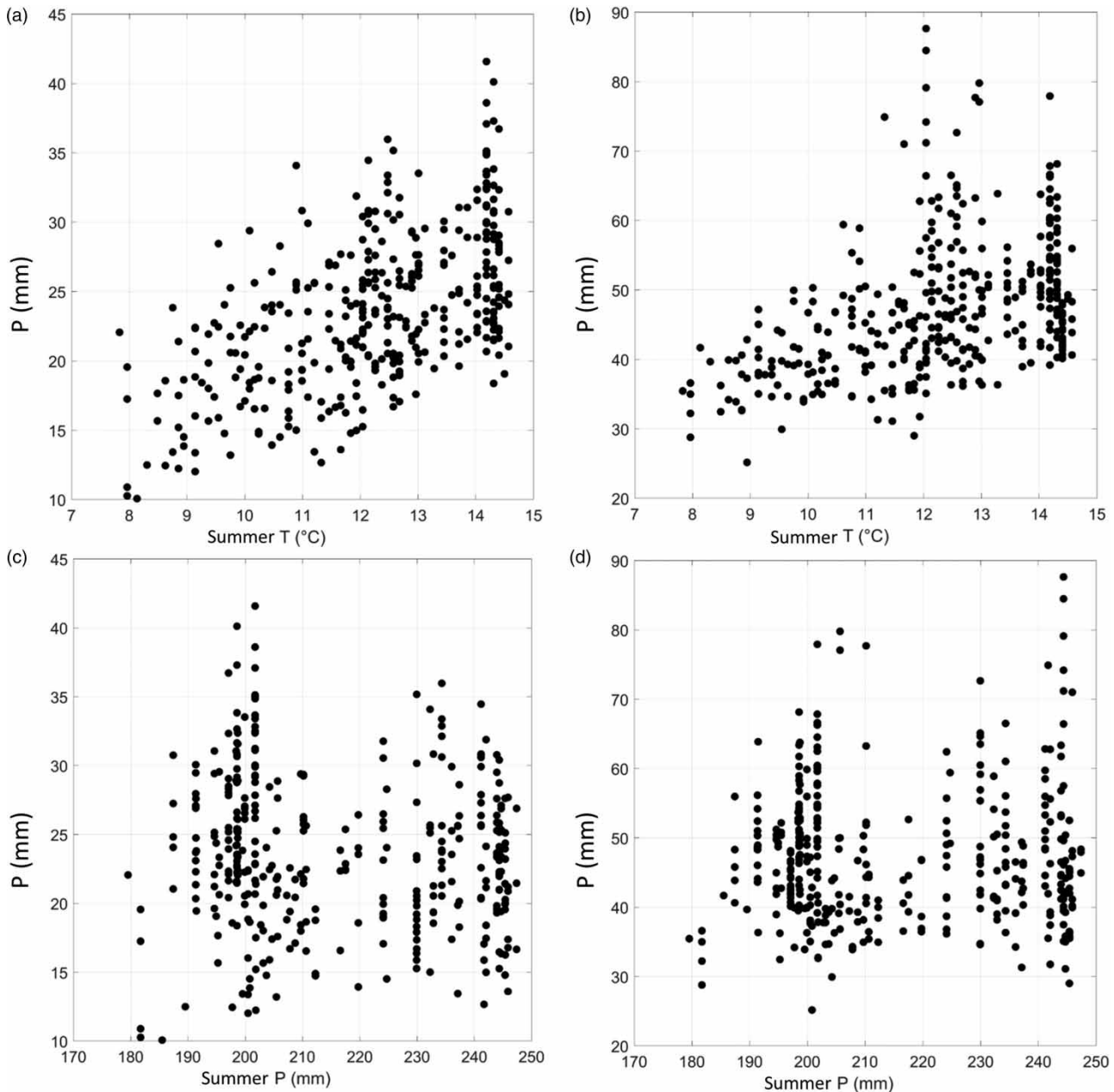
Figure 5 | Estimated 10-year rainfall P as a function of average summer temperature for the following durations: (a) 1 h and (b) 12 h. Estimated 10-year rainfall as a function of total summer precipitation for the following durations: (c) 1 h and (d) 12 h.

The grid at 1 h (Figure 7(a)), interpolated from the point values in Figure 6(a), illustrates the complex 1-h pattern with early dates in Sweden and Finland (especially in the northern parts), late dates in western Norway, with the Baltic states and Denmark somewhere in between. In the gridded data, the date interval ranges from doy 206 (25 July) to doy 223 (11 August), i.e., spanning just over 2 weeks. This is a shorter period than in Figure 6(c), and this reduction is caused by smoothing of the substantial spatial variability (Figure 6(a)) in the interpolation to grid. Thus, the gridded data must be interpreted (and used) with caution, but we believe the overall pattern is sensibly and credibly represented. At duration 12 h (Figure 7(b)), the overall pattern is more clear with a distinct longitudinal dependence, as suggested in Figure 6(b), and more than 1 month between the earliest date (doy 208; 27 July) and the latest date (doy 245; 2 September) (Figure 7(b)).
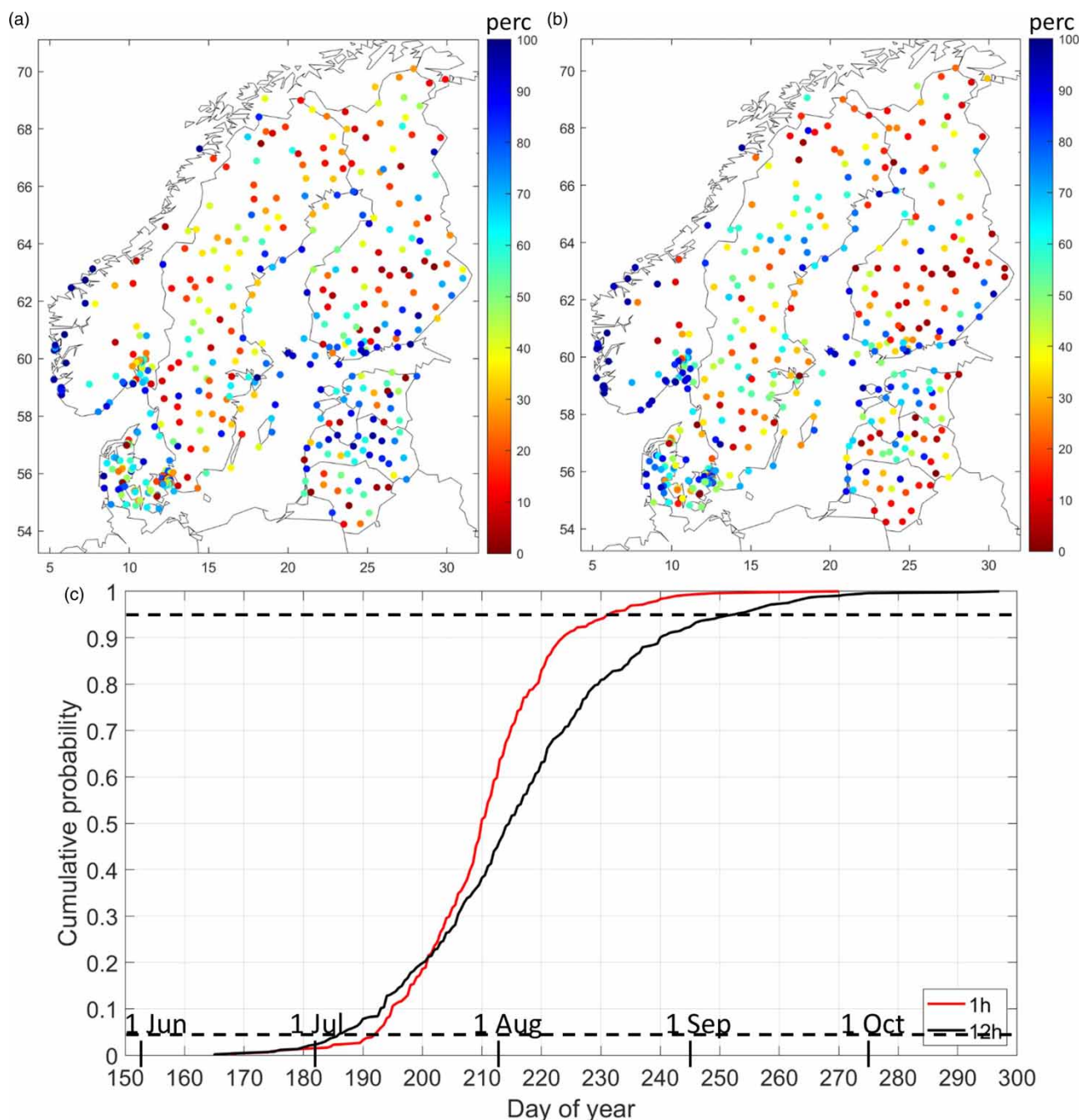
Figure 6 | Maximum dates (day of year) for the following durations: (a) 1 h and (b) 12 h (zoom-ins on DK are available in Supplement, Figure S5). The colours represent the percentile (perc) of the entire frequency distributions. The dashed lines in (c) illustrate the limits of the central 90%.

Finally, we look at trends in Norway and Denmark where almost 40 years of data were available for the study. The ratio of 10-year return levels estimated from the period 2000–2018 to the corresponding values estimated from the period 1980–1999 are examined; a positive value indicates a positive trend, and vice versa (Figure 8).

At duration 1 h, the stations in Norway show a mixed picture with around half of the stations indicating an increase and half a decrease (Figure 8(a)). A longitudinal dependence is weakly suggested, with a decrease in western Norway and an increase in eastern Norway, although this pattern may also be related to other geographical features. In Denmark, there is a more consistent signal of a positive trend, with only a few stations indicating a (very weakly) negative trend. Also here,
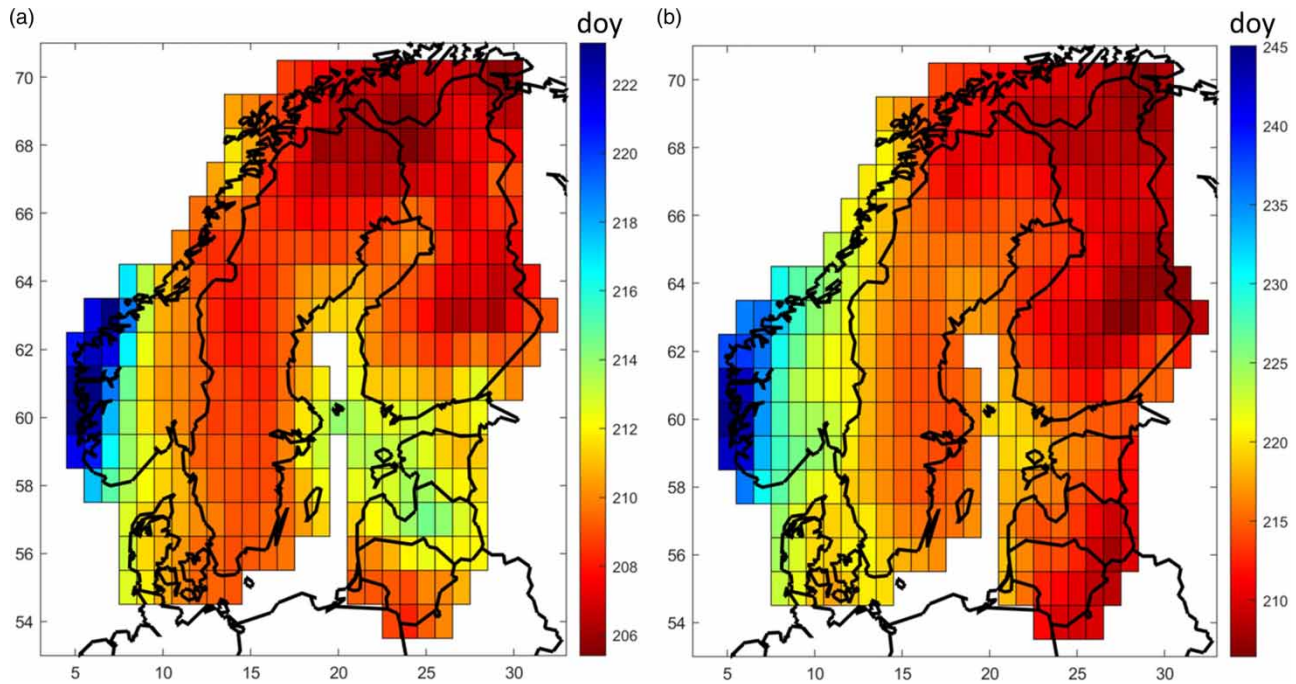
Figure 7 | Gridded (interpolated) maximum dates (day of year) for the following durations: (a) 1 h and (b) 12 h.
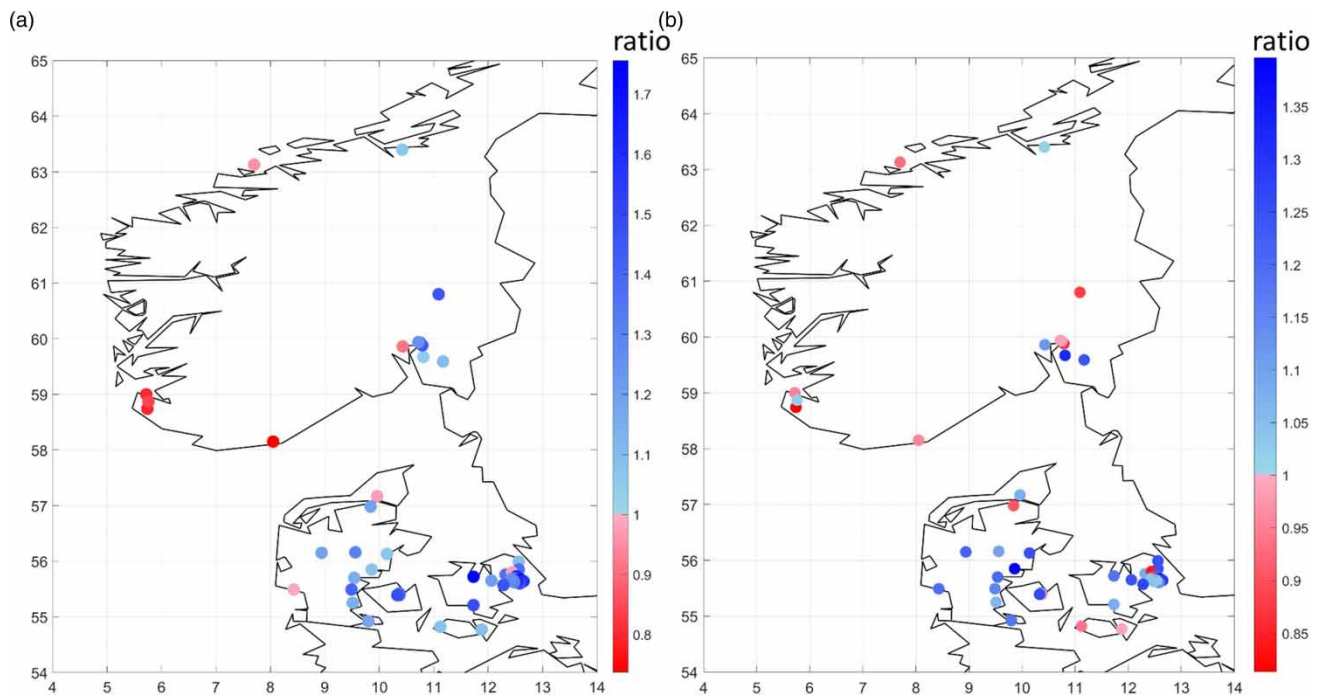

Figure 8 | Ratio of the 10-year value calculated from the period 2000 to 2018 to the value calculated from the period 1980 to 1999 for the following durations: (a) 1 h and (b) 12 h (zoom-ins on DK are available in Supplement, Figure S6).

a weak longitudinal dependence is indicated. The picture is overall similar at duration 12 h, with mixed signals in Norway and a general increase in Denmark.

The results in Figure 8 may be compared with the analyses of trends in annual daily maxima by Dyrrdal *et al.* (2021), within the same domain as used in this study. Concerning Norway, it is there suggested that the picture is quite mixed along the

coast, with stations indicating both positive and negative trends, whereas in central south Norway there is a consistent and clear signal of increasing trends. Thus, it may be that the predominantly negative trends found along the Norwegian coast here are coincidental and not representative of south-western Norway. Concerning Denmark, the predominantly positive trends found in this study are in good agreement with Gregersen *et al.* (2013), who found that both time and mean annual precipitation were significant covariates when setting up a non-stationary model for the full Danish sub-daily data set.

DISCUSSION

One limitation of the present study is clearly the different devices used for observing rainfall in the countries involved (Table 1) as well as the different procedures used for post-processing and quality assurance. Even so, the results appear overall spatially consistent, without obvious discontinuities along borders, and in line with expectations based on existing knowledge and previous studies. Therefore, we believe that the results and the open data (*i*) well represent the character of sub-daily rainfall extremes in the region and (*ii*) can be used for different applications (see further Conclusions).

One key aspect of extreme value analyses of short-duration rainfall is the choice of probability distribution and the associated data used to represent the extremes. Two common approaches are (*i*) GEV distribution fitted to AM (AM) and (*ii*) Generalized Pareto (GP) distribution fitted to partial duration (a.k.a. peak over threshold) series (PDS) (e.g. Madsen *et al.* 1997). In this study, we use GEV/AM because of convenience and unambiguity, to facilitate for the contributing partners. To make a limited assessment of the impact of this choice, both GEV/AM and GP/PDS were applied to the data from Denmark. The results indicated some 5–10% higher 10-year return levels with GP/PDS and we attribute this difference primarily to the inclusion of higher values by PDS. Still the difference is limited, i.e., the choice of approach has a limited impact on the return levels.

The results in terms of 10-year return levels across the domain, as expressed in the gridded open data (Figure 3), may be compared with available national analyses and estimates, even though these have been generally performed using different methods and procedures.

- Denmark: Madsen *et al.* (2017) provide return levels for Denmark. At duration 1 h, they found a 10-year rainfall of 24.9 $\pm$ 3.3 mm, which is in good agreement with the level in this study. They, however, found a tendency to higher values in the western part of Denmark, whereas we find a weak opposite tendency here. At 12 h, our values are close to the upper limit of their estimation which is 46.7 $\pm$ 4.0 mm.
- Estonia: In Estonia, the rainfall return levels are assumed to be almost constant with very low variability across Estonia for short durations. From observations in the period 2011–2020, the 10-year 1-h level is estimated to be 27 mm which well agrees with our estimate. Recent estimations from polarimetric radar data, however, suggest a value of 32 mm (Voormansik *et al.* 2021).
- Finland: The 10-year 1-h estimate for Finland is 22.8 mm which is based on measurements at two in-situ stations located in the south and north of Finland (Katajisto 1969). This value has later been confirmed by Aaltonen *et al.* (2008), using radar measurements over the whole of Finland between 2000 and 2005, and Saku *et al.* (2016), who found that the probability of heavy precipitation events is lower in northern Finland compared to the south. Both the value and the gradient are well in line with the results found here. For duration 6 h, the estimates for 10-year return levels are 44 mm for southern Finland (Jokioinen) and 26 mm for northern Finland (Sodankylä) (Venäläinen *et al.* 2007). In this study we find a smaller variation across Finland, approximately between 33 and 37 mm.
- Latvia, Lithuania: Here, we are not aware of any previous investigation with which to meaningfully compare.
- Norway: For Norway, the spatial distribution in Figure 3 is very similar to maps created using the method in Dyrrdal *et al.* (2015), although the coarser resolution allows for less spatial variability. The highest values, in the coastal southeast and the western coast of southern Norway, respectively, are also in accordance. However, the method by Dyrrdal *et al.* (2015) produces smaller values in the north, down to 10–12 mm and around 35 mm for 1- and 12-h duration, respectively.
- Sweden: Based on an analysis of the same data base as used in this study, Olsson *et al.* (2019) proposed a division of Sweden into four regions – south-western, south-eastern, central and northern Sweden – with different depth–duration–frequency (DDF) statistics. Visually, these regions are well reflected in the gridded 10-year values (Figure 3). In terms of the return levels, these are generally in good agreement although in the northern region the national values are somewhat lower.

These results to some extent complement the recent study of sub-daily rainfall extremes in Europe by Poschlod *et al.* (2021). In Denmark, Finland, Norway and Sweden, Poschlod *et al.* (2021) use effectively the same national data sets that are used in

the above evaluation; thus our findings are valid also with respect to their data. They, however, found a distinct deviation between eastern Norway and western Sweden, explained by different network densities as well as analysis methods. This discontinuity is not clearly visible in our results. Furthermore, our study is complementary by including the Baltic states.

During the study, some attempts were made to develop generalized mathematical descriptions able to estimate the return level at an arbitrary point within the domain. One approach was to correlate the return level to geographical and hydro-meteorological predictors, as shown in Figures 4 and 5. Although some dependence was found, it did not turn out sufficient for meaningful estimation. Another attempt was to perform regional clustering based on estimated GEV-parameters in combination with latitude/longitude/altitude-coordinates, similarly to Olsson *et al.* (2019) for Sweden. The resulting clusters were, however, not considered sufficiently distinct or consistent for further analysis and application.

CONCLUSIONS

Sub-daily rainfall observations from 543 meteorological stations in the Nordic–Baltic region during 2000–2018 were collected, quality-controlled and consistently analyzed to estimate extreme values for different durations (1–12 h) and return periods (5, 10 and 20 years) as well as their time of occurrence. The results reflect the highly heterogeneous rainfall climate in the region, with longitudinal and latitudinal gradients as well as local variability. The results are overall in good agreement with earlier, national investigations although some discrepancies exist. Trend analyses in Norway and Denmark indicated predominantly positive trends in the period 1980–2018, in line with previous investigations. Gridded data sets with 10-year return levels and dates of occurrence (of AM) are provided open access (Olsson *et al.* 2021b).

We see different potential applications of the results and the open data sets. One is for evaluation of climate models. Currently very high-resolution convection-permitting regional climate models are being developed and evaluated, and they generally show a distinctly improved performance as compared with earlier, lower-resolution models (e.g. Lind *et al.* 2020; Olsson *et al.* 2021a). The open data sets are currently used for additional evaluation and we foresee further similar applications in the future. Another potential application concerns the prospect of Nordic–Baltic harmonization with respect to extreme rainfall statistics for, e.g., engineering design. Currently the situation is rather diversified, e.g., with different recommended return levels and warning thresholds based on different analysis methods.

Finally, we encourage further efforts towards international exchange of sub-daily rainfall observations as well as consistent regional analyses. An increase in the frequency and magnitude of sub-daily rainfall extremes is a key consequence of global warming, with serious implications for society. We need to attain the best possible knowledge on which rainfall extremes are to be expected in present as well as future climate.

ACKNOWLEDGEMENTS

DATA AVAILABILITY STATEMENT

All relevant data are available from an online repository: https://archive.norstore.no/pages/public/datasetDetail.jsf?id=10.11582/2021.00094. Gridded values of return levels (Figure 3) and maximum dates (Figure 7) are provided open access through NIRD Research Data Archive (Olsson *et al.* 2021b).

REFERENCES

Aaltonen, J., Hohti, H., Jylhä, K., Karvonen, T., Kilpeläinen, T., Koistinen, J., Kotro, J., Kuitunen, T., Ollila, M., Parvio, A., Pulkkinen, S., Silander, J., Tiihonen, T., Tuomenvirta, H. & Vajda, A. 2008 *Rankkasateet ja Taajamatulvat (Heavy Rains and Floods in Urban Areas)*. Tech. Rep., Finnish Environment Institute, Helsinki, Finland, p. 126.

Alber, R., Jaagus, J. & Oja, P. 2015 Diurnal cycle of precipitation in Estonia. *Estonian Journal of Earth Sciences* **64** (4), 305.

Arnbjerg-Nielsen, K. 2006 Significant climate change of extreme rainfall in Denmark. *Water Science and Technology* **54** (6–7), 1–8.

Arnbjerg-Nielsen, K., Leonardsen, L. & Madsen, H. 2015 Evaluating adaptation options for urban flooding based on new high-end emission scenario regional climate model simulations. *Climate Research* **64** (1), 73–84.

Bakkehøi, S., Øien, K. & Førland, E. J. 1985 An automatic precipitation gauge based on vibrating-wire strain gauges. *Hydrology Research* **16** (4), 193–202.

Beck, H. E., Zimmermann, N. E., McVicar, T. R., Vergopolan, N., Berg, A. & Wood, E. F. 2018 Present and future Köppen-Geiger climate classification maps at 1-km resolution. *Scientific Data* **5** (1), 1–12.

Berg, P., Christensen, O. B., Klehmet, K., Lenderink, G., Olsson, J., Teichmann, C. & Yang, W. 2019 Summertime precipitation extremes in a EURO-CORDEX 0.11 ensemble at an hourly resolution. *Natural Hazards and Earth System Sciences* **19** (4), 957–971.

Coles, S. 2001 *An Introduction to Statistical Modelling of Extreme Values*. Springer-Verlag, London, UK.

Dahlström, B. 1979 *Regional Fördelning av Nederbördsintensitet – en Klimatologisk Analys (Regional Distribution of Precipitation Intensity – A Climatological Analysis)*. Report R18:1979, BRF, Stockholm, Sweden.

Dahlström, B. 2021 Cloud physical and climatological factors for the determination of rain intensity. *Water* **13** (16), 2292.

Dyrrdal, A. V., Lenkoski, A., Thorarinsdottir, T. L. & Stordal, F. 2015 Bayesian hierarchical modeling of extreme hourly precipitation in Norway. *Environmetrics* **26** (2), 89–106.

Dyrrdal, A. V., Olsson, J., Toivonen, E., Arnbjerg-Nielsen, K., Poste, P., Aniskevica, S., Thorndahl, S., Førland, E., Wern, L., Maciulyte, V. & Mäkelä, A. 2021 Observed changes in heavy daily precipitation over the Nordic-Baltic region. *Journal of Hydrology Regional Studies* **38**, 100965.

Gregersen, I. B., Madsen, H., Rosbjerg, D. & Arnbjerg-Nielsen, K. 2013 A spatial and nonstationary model for the frequency of extreme rainfall events. *Water Resources Research* **49** (1), 127–136.

Hersbach, H., Bell, B., Berrisford, P., Hirahara, S., Horányi, A., Muñoz-Sabater, J., Nicolas, J., Peubey, C., Radu, R., Schepers, D., Simmons, A., Soci, C., Abdalla, S., Abellan, X., Balsamo, G., Bechtold, P., Biavati, G., Bidlot, J., Bonavita, M., De Chiara, G., Dahlgren, P., Dee, D., Diamantakis, M., Dragani, R., Flemming, J., Forbes, R., Fuentes, M., Geer, A., Haimberger, L., Healy, S., Hogan, R. J., Hólm, E., Janisková, M., Keeley, S., Laloyaux, P., Lopez, P., Lupu, C., Radnoti, G., de Rosnay, P., Rozum, I., Vamborg, F., Villaume, S. & Thépaut, J. N. 2020 The ERA5 global reanalysis. *Quarterly Journal of the Royal Meteorological Society* **146** (730), 1999–2049.

Hosking, J. R. 1990 L-moments: analysis and estimation of distributions using linear combinations of order statistics. *Journal of the Royal Statistical Society: Series B (Methodological)* **52** (1), 105–124.

Hosking, J. R. & Wallis, J. R. 1987 Parameter and quantile estimation for the generalized pareto distribution. *Technometrics* **29** (3), 339–349.

IPCC 2021 Summary for Policymakers. In: *Climate Change 2021: The Physical Science Basis. Contribution of Working Group I to the Sixth Assessment Report of the Intergovernmental Panel on Climate Change* (MassonDelmotte, V., Zhai, P., Pirani, A., Connors, S. L., Péan, C., Berger, S., Caud, N., Chen, Y., Goldfarb, L., Gomis, M. I., Huang, M., Leitzell, K., Lonnoy, E., Matthews, J. B. R., Maycock, T. K., Waterfield, T., Yelekçi, O., Yu, R. & Zhou, B., eds.). Cambridge University Press, Cambridge, UK.

Jørgensen, H. K., Rosenørn, S., Madsen, H. & Mikkelsen, P. S. 1998 Quality control of rain data used for urban runoff systems. *Water Science and Technology* **37** (11), 113–120.

Katajisto, R. 1969 *Rankkasateiden Voimakkuus ja Toistumistiheys Suomessa (The Intensity and Frequency of the Heavy Precipitation in Finland)*. Rakennushallituksen tiedotuksia 1969. (Bulletins by National Board of Public Building in 1969).

Lewis, E., Fowler, H., Alexander, L., Dunn, R., McClean, F., Barbero, R., Guerreiro, S., Li, X.-F. & Blenkinsop, S. 2019 GSDR: a global sub-daily rainfall dataset. *Journal of Climate* **32** (15), 4715–4729.

Lind, P., Belušić, D., Christensen, O. B., Dobler, A., Kjellström, E., Landgren, O., Lindstedt, D., Matte, D., Pedersen, R. A., Toivonen, E. & Wang, F. 2020 Benefits and added value of convection-permitting climate modeling over Fenno-Scandinavia. *Climate Dynamics* **55** (7), 1893–1912.

Lutz, J., Grinde, L. & Dyrrdal, A. V. 2020 Estimating rainfall design values for the city of Oslo, Norway – comparison of methods and quantification of uncertainty. *Water* **12** (6), 1735.

Madsen, H., Rasmussen, P. F. & Rosbjerg, D. 1997 Comparison of annual maximum series and partial duration series methods for modeling extreme hydrologic events: 1. At-site modeling. *Water Resources Research* **33** (4), 747–757.

Madsen, H., Gregersen, I. B., Rosbjerg, D. & Arnbjerg-Nielsen, K. 2017 Regional frequency analysis of short duration rainfall extremes using gridded daily rainfall data as co-variate. *Water Science and Technology* **75** (8), 1971–1981.

Müller, M., Homleid, M., Ivarsson, K. I., Køltzow, M. A., Lindskog, M., Midtbø, K. H., Andrae, U., Aspelien, T., Berggren, L., Bjørge, D., Dahlgren, P., Kristiansen, J., Randriamampianina, R., Ridal, M. & Vignes, O. 2017 AROME-MetCoOp: A Nordic convective-scale operational weather prediction model. *Weather and Forecasting* **32** (2), 609–627.

Olsson, J., Södling, J., Berg, P., Wern, L. & Eronn, A. 2019 Short-duration rainfall extremes in Sweden: a regional analysis. *Hydrology Research* **50** (3), 945–960.

Olsson, J., Du, Y., An, D., Uvo, C. B., Sörensen, J., Toivonen, E. & Dobler, A. 2021a An analysis of (sub-) hourly rainfall in convection-permitting climate simulations over southern Sweden from a user's perspective. *Frontiers in Earth Science* **9**, 516.

Olsson, J., Dyrrdal, A. V., Toivonen, E., Södling, J., Aniskeviča, S., Arnbjerg-Nielsen, K., Førland, E., Mačiulytė, V., Mäkelä, A., Post, P., Thorndahl, S. L. & Wern, L. 2021b Gridded return levels and maximum dates of short-duration rainfall extremes in the Nordic-Baltic region (data set). *NIRD Research Data Archive* doi: 10.11582/2021.00094.

Poschlod, B., Ludwig, R. & Sillmann, J. 2021 Ten-year return levels of sub-daily extreme precipitation over Europe. *Earth System Science Data* **13** (3), 983–1003.

Saku, S., Mäkelä, A., Jylhä, K. & Niinimäki, N. 2016 *Lyhytkestoisten sateiden rankkuus ja toistuvuusaika Suomessa (The Intensity and Frequency of the Short-Duration Rainfall in Finland)*. Finnish Meteorological Institute, Helsinki, p. 15.

Smith, A., Lott, N. & Vose, R. 2011 The integrated surface database: recent developments and partnerships. *Bulletin of the American Meteorological Society* **92** (6), 704–708.

Sokol, Z., Szturc, J., Orellana-Alvear, J., Popová, J., Jurczyk, A. & Célleri, R. 2021 The role of weather radar in rainfall estimation and its application in meteorological and hydrological modelling – A review. *Remote Sensing* **13** (3), 351.

Sorteberg, A., Lawrence, D., Dyrrdal, A. V., Mayer, S. & Engeland, K. 2018 *Climatic Changes in Short Duration Extreme Precipitation and Rapid Onset Flooding – Implications for Design Values*. Report 1/2018. Norwegian Centre for Climate Services.

Thorndahl, S., Einfalt, T., Willems, P., Nielsen, J. E., Veldhuis, M. C. T., Arnbjerg-Nielsen, K., Rasmussen, M. R. & Molnar, P. 2017 Weather radar rainfall data in urban hydrology. *Hydrology and Earth System Sciences* **21** (3), 1359–1380.

Venäläinen, A., Saku, S., Kilpeläinen, T., Jylhä, K., Tuomenvirta, H., Vajda, A., Räisänen, J. & Ruosteenoja, K. 2007 *Sään ääri-Ilmiöistä Suomessa. (Aspects About Climate Extremes in Finland)*. Reports 2007:4, Finnish Meteorological Institute, Helsinki, p. 81.

von Scherling, M., Jonsson, C., Andersson, J., van de Beek, R. & Hansryd, J. 2021 Simulering av avloppsflöden med regndata från mobiltelefonnät i Stockholm (Simulating urban drainage flows with rainfall data derived from mobile phone networks in Stockholm). *Journal of Water Management and Research (VATTEN)* **77** (2), 91–104.

Voormansik, T., Cremonini, R., Post, P. & Moisseev, D. 2021 Evaluation of the dual-polarization weather radar quantitative precipitation estimation using long-term datasets. *Hydrology and Earth System Sciences* **25**, 1245–1258. https://doi.org/10.5194/hess-25-1245-2021, 2021.

Willems, P., Olsson, J., Arnbjerg-Nielsen, K., Beecham, S., Pathirana, A., Gregersen, I. B., Madsen, H. & Nguyen, V. T. V. 2012 *Impacts of Climate Change on Rainfall Extremes and Urban Drainage Systems*. IWA Publishing, London.

WMO 2009 *Manual for Estimation of Probable Maximum Precipitation*. Publication No. 1045, World Meteorological Organization, Geneva, Switzerland.

Young, C. B. & McEnroe, B. M. 2003 Sampling adjustment factors for rainfall recorded at fixed time intervals. *Journal of Hydrologic Engineering* **8** (5), 294–296.